Ferromagnetic quantum criticality in the quasi-one-dimensional heavy fermion metal $YbNi_4P_2$

2011 New J. Phys. 13 103014

(http://iopscience.iop.org/1367-2630/13/10/103014)

New Journal of Physics
The open-access journal for physics

Ferromagnetic quantum criticality in the quasi-one-dimensional heavy fermion metal $YbNi_4P_2$

C Krellner[1], S Lausberg, A Steppke, M Brando, L Pedrero, H Pfau, S Tencé, H Rosner, F Steglich and C Geibel

Max Planck Institute for Chemical Physics of Solids, D-01187 Dresden, Germany
E-mail: krellner@cpfs.mpg.de

New Journal of Physics **13** (2011) 103014 (12pp)
Received 19 May 2011
Published 12 October 2011
Online at http://www.njp.org/
doi:10.1088/1367-2630/13/10/103014

Abstract. We present a new Kondo-lattice system, $YbNi_4P_2$, which is a clean heavy-fermion metal with a severely reduced ferromagnetic (FM) ordering temperature at $T_C = 0.17$ K, evidenced by distinct anomalies in susceptibility, specific heat and resistivity measurements. The FM nature of the transition, with only a small ordered moment of $\sim 0.05\mu_B$, is established by a diverging susceptibility at T_C with huge absolute values in the ferromagnetically ordered state, severely reduced by small magnetic fields. Furthermore, $YbNi_4P_2$ is a stoichiometric system with a quasi-one-dimensional crystal and electronic structure and strong correlation effects which dominate the low-temperature properties. This is reflected by a stronger-than-logarithmically diverging Sommerfeld coefficient and a linear-in-T resistivity above T_C, which cannot be explained by current theoretical predictions. These exciting characteristics are unique among all correlated electron systems and make this an interesting material for further in-depth investigations.

Phase transitions are one of the most fascinating phenomena and a central topic in solid-state physics. While classical phase transitions driven by thermal fluctuations have been extensively studied, the current interest is in continuous quantum phase transitions, which occur at zero temperature and are caused by collective quantum fluctuations between competing ground

[1] Author to whom any correspondence should be addressed.

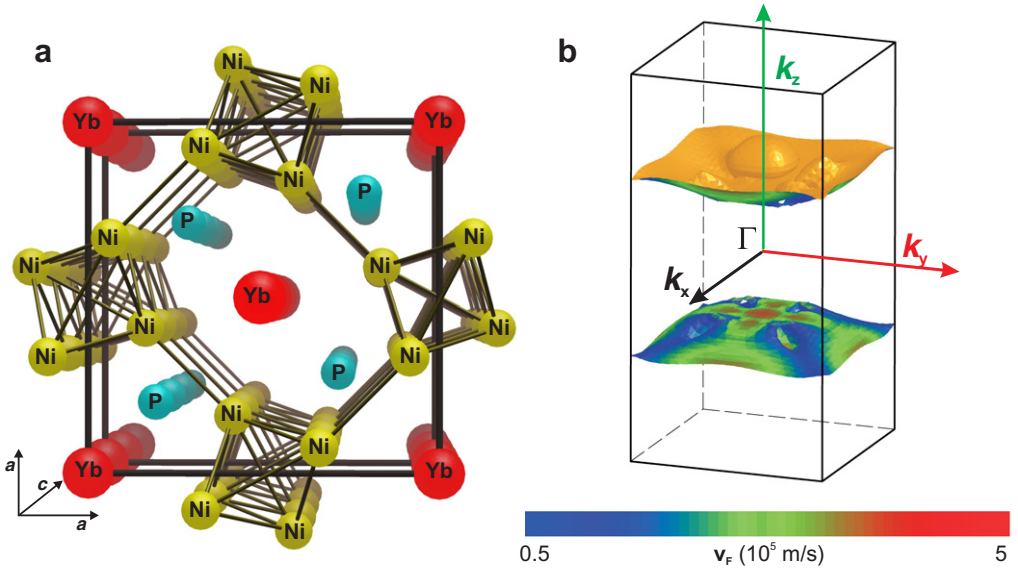

Figure 1. Quasi-1D crystal and electronic structure of $YbNi_4P_2$. (a) Stereoscopic view of the tetragonal crystal structure along c with the Yb chains located in the channels between chains of edge-connected Ni tetrahedra. Details of the structural refinement of our samples are given in appendix B. (b) Topology of one of the uncorrelated Fermi surfaces with the most pronounced 1D character manifested in two nearly flat sheets, well separated along k_z. Note that the viewing direction is rotated by 90° compared to the crystal structure. The size of the Fermi velocity, v_F, of the mainly Ni-3d states dominating the density of states at E_F is colour-coded.

states [1]. Namely, the emergence of intriguing new states of matter at such a quantum critical point (QCP) was explored in great detail in Lanthanide-based heavy-fermion systems [2–6]. However, despite these studies, over more than two decades, no 4f-based material with a ferromagnetic (FM)-to-paramagnetic quantum phase transition has been found. The reason for this lapse remains hotly debated [7–9]. Here, we present a new heavy-fermion metal, $YbNi_4P_2$, which indeed presents FM quantum criticality above a low-lying FM transition temperature.

Intermetallic pnictides have recently become a focus of attention in the solid-state physics community as a result of the discovery of high-temperature superconductivity in the RFeAsO (R = rare earth) and AFe_2As_2 (A = alkali metal) systems with different substitutions (for a review, see, e.g., [10]). While these compounds present a pronounced quasi-two-dimensional (quasi-2D) character, the pnictides crystallizing in the $ZrFe_4Si_2$ structure type are quasi-1D and have been poorly investigated [11–13]. In figure 1(a), we present the tetragonal $ZrFe_4Si_2$ structure type ($P4_2/mnm$) of $YbNi_4P_2$, which can be viewed as isolated chains (along the c-direction) of edge-connected Ni tetrahedra, with adjacent chains linked by Ni–Ni bonds between the corners of the tetrahedra. The Yb atoms are located in the channels between these Ni tetrahedral chains. The quasi-1D character in the Yb and in the Ni network, as well as the geometrical frustration between neighbouring Yb chains that are shifted by $c/2$, are prone to cause strong quantum fluctuations if Yb is magnetic (Yb^{3+}).

Previously, only a susceptibility curve at high temperatures of an impure $YbNi_4P_2$ sample was reported by Deputier *et al* [14]. These authors suggested magnetic Yb^{3+} ions and a

non-magnetic contribution of the 'Ni_4P_2' sublattice revealed by weak Pauli paramagnetism in the reference compound YNi_4P_2, in contrast to the first measurements by Chikhrij *et al* [15] that suggested a ferromagnetically ordered sublattice above room temperature, most probably due to Ni impurity phases. We succeeded in preparing single-phase $YbNi_4P_2$ polycrystals. Our susceptibility measurements, $\chi(T)$, indicate clear Curie–Weiss behaviour between 50 and 400 K with a Weiss temperature, $\Theta_W = -30$ K, and an effective moment, $\mu_{eff} = 4.52\mu_B$, due to magnetic Yb^{3+} ions, thus supporting the absence of a Ni moment. The lattice parameters $a = 7.0565(2)$ Å and $c = 3.5877(1)$ Å refined by simple least squares fitting agree well with the reported structure data [16]. A complete structure refinement based on tiny single crystals is given in appendix B.

To gain insight into the electronic structure of $YbNi_4P_2$, we performed band structure calculations of the 'Ni_4P_2' sublattice. For this purpose, the $4f^{13}$ electrons are frozen as core states and are not allowed to hybridize with the conduction electrons as the strong Coulomb correlations of the Yb 4f electrons would give incorrect results in the mean-field approximation. Two main issues can be inferred from the uncorrelated band structure: firstly, the three main Fermi surfaces have a predominantly 1D character: the most prominent one is visualized in figure 1(b) with two nearly flat sheets (well separated along k_z), which is typical for a 1D system in real space. Therefore, not only the crystal structure, but also the electronic structure suggest that $YbNi_4P_2$ is a quasi-1D system, unique among Kondo-lattice systems. Secondly, spin-polarized calculations clearly demonstrate the absence of Ni-related magnetism in $YbNi_4P_2$, although the main contributions to the density of states at the Fermi energy, E_F, result from Ni-3d states.

The temperature dependence of the resistivity, $\rho(T)$, and the Seebeck coefficient, $S(T)$, between 2 and 300 K (figure 2) evidence that $YbNi_4P_2$ is a Kondo lattice with strong interactions between 4f and conduction electrons. $\rho(T)$ decreases linearly down to 50 K with a room temperature value of $\rho_{300\,K} \cong 120\,\mu\Omega$ cm, before dropping rapidly below 20 K due to the onset of coherent Kondo scattering. The correspondingly large residual resistivity ratio, $\rho_{300\,K}/\rho_0 = 50$, reveals a long electronic mean free path at low T, which demonstrates the high quality of our polycrystalline sample. Assuming that the linear decrease down to 50 K dominantly results from phonon scattering, the magnetic part of the resistivity reveals a typical Kondo maximum around 30 K. The presence of strong hybridization between the 4f and the conduction electrons in $YbNi_4P_2$ is further supported by thermopower measurements (see figure 2(b)). $S(T)$ is negative within the whole temperature range investigated, a fact that is well established in Yb-based Kondo lattices. Moreover, $S(T)$ presents a pronounced minimum at 35 K with absolute values as high as 40 μV K^{-1}. Extrema in $\rho(T)$ and $S(T)$ originate from Kondo scattering on the ground and the excited crystal electric field (CEF) levels [17]. Since the CEF scheme of $YbNi_4P_2$ is at present unknown, a reliable estimate of the Kondo energy scale, T_K (for the lowest-lying CEF Kramers doublet), can only be obtained by means of the magnetic entropy calculated from the specific heat data, discussed below. At 4 K, the entropy reaches $0.5R \ln 2$, establishing a doublet ground state with $T_K \cong 8$ K.

We now turn to the exciting low-temperature properties of $YbNi_4P_2$ presented in figure 3. Below $T = 10$ K, the ac susceptibility, χ, increases and nearly diverges towards $T_C = 0.17$ K where the 4f moments undergo an FM phase transition. The temperature and magnetic field dependences of χ are distinctive for a ferromagnetically ordered material (see figure 3(a)). The FM nature of the magnetic phase is one of our key results since the majority of the currently known Kondo lattices order antiferromagnetically. Most prominent are the huge absolute values

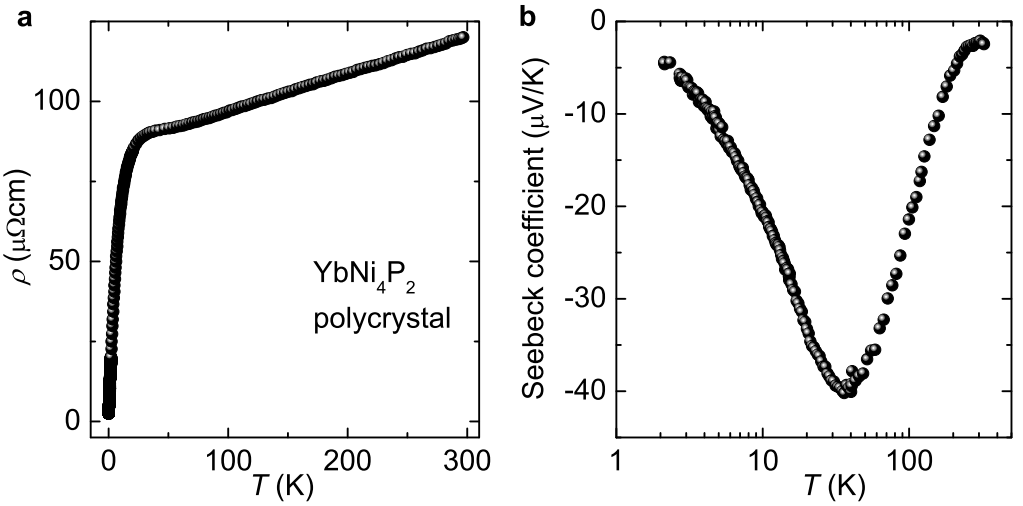

Figure 2. $YbNi_4P_2$: a metallic Kondo lattice. (a) The temperature dependence of the resistivity is overall metallic with a pronounced drop below 30 K, marking the onset of coherent Kondo scattering. The high residual resistivity ratio, $\rho_{300\,\mathrm{K}}/\rho_0 = 50$, demonstrates that our polycrystalline sample is very clean. (b) The temperature dependence of the Seebeck coefficient shows a distinct minimum at 35 K, characteristic of Yb-based Kondo lattices. The large absolute values near this minimum are commonly ascribed to a strongly energy-dependent quasi-particle density of states at E_F.

of χ in zero magnetic field. To assess the magnitude of the divergence at T_C, we scaled the right-hand ordinate of figure 3(a) to the dimensionless volume susceptibility, i.e. $\chi_{vol} = \chi_{mol}/V_{mol}$ with the molar volume, $V_{mol} = 53.8 \times 10^{-6}\,m^3\,mol^{-1}$, yielding a value at T_C of $\chi_{vol} = 3.3$. The fact that the magnetic ordering temperature of the Yb moments is so strongly reduced results primarily from the pronounced Kondo interactions. Further evidence for ferromagnetism comes from the very pronounced field dependence of the susceptibility, which is suppressed by a factor of two, applying a small field of $B = 0.5$ mT. This makes an antiferromagnetic (AFM) or helical order rather unlikely. However, we cannot completely exclude a magnetic ordering vector with a very tiny q, but also in such a case the FM interaction would be the most dominant one. For $B \geqslant 5$ mT, a broad maximum develops in $\chi(T)$, which shifts to higher temperatures with increasing fields due to the energetic stabilization of the FM ground state in a magnetic field. In the inset of figure 3(a), we present the magnetization data below and above T_C obtained from the same sample, confirming the FM nature of the magnetic transition. At 60 mK, the magnetization is strongly nonlinear and increases steeply with field below $B = 150$ mT due to a small ordered FM moment of $M_{ord} \cong 0.05\mu_B$, followed by a second kink at $B = 3.5$ T, which represents either the rotation of the FM moments along the magnetic hard direction (perpendicular to the direction of the FM moment) or complete suppression of the Kondo screening. Above T_C, both anomalies are absent and the polarized moment amounts to $M \cong 0.6\mu_B$ at $B = 5$ T. More detailed magnetization measurements at low fields are presented in the appendix A.

Specific heat data, shown in figure 3(b), strongly confirm that $YbNi_4P_2$ is a magnetically ordered heavy-fermion system. A sharp λ-type anomaly is observed at T_C, establishing a second-order phase transition to the FM phase. Well below T_C, a huge Sommerfeld coefficient,

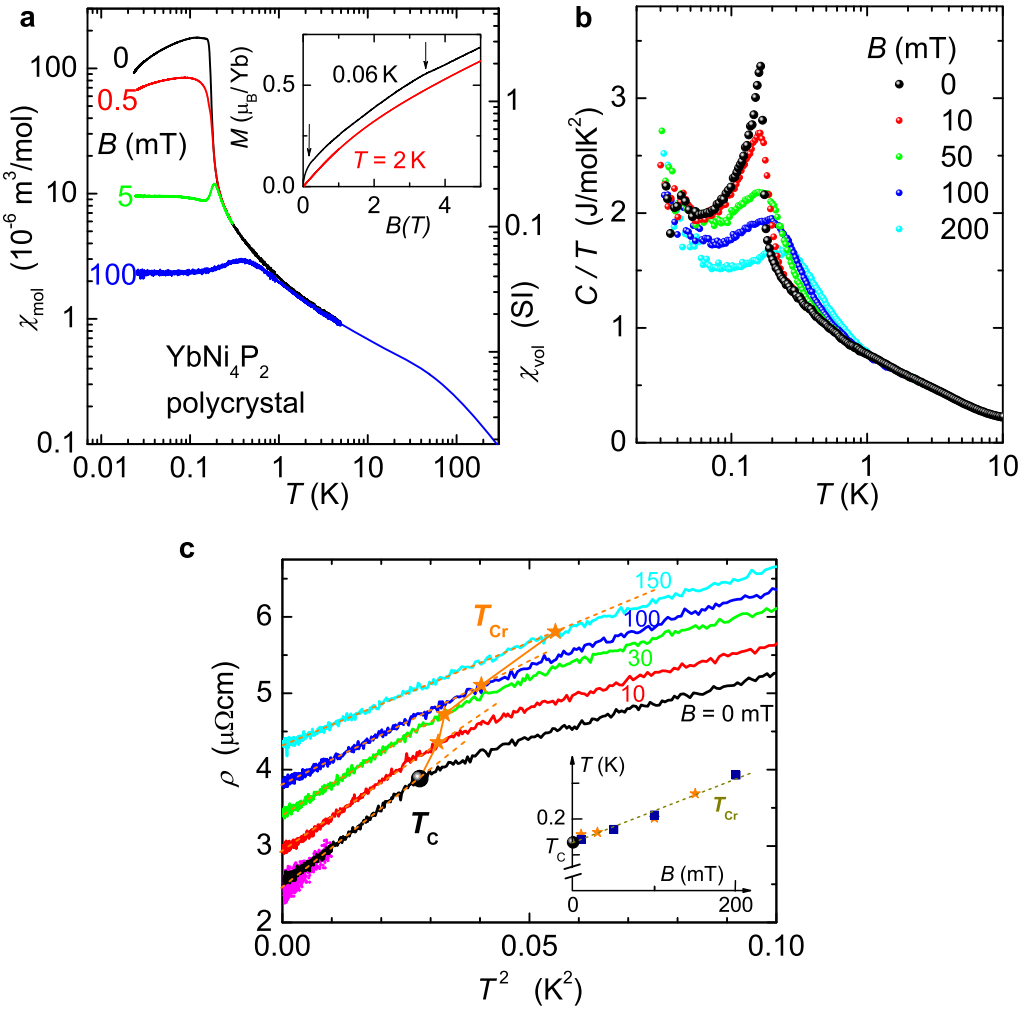

Figure 3. Low-lying FM transition at $T_C = 0.17$ K in $YbNi_4P_2$. (a) Temperature-dependent ac susceptibility, $\chi_{mol}(T)$, at selected magnetic fields reveals an FM phase transition at T_C with very high absolute values. The right-hand ordinate is divided by the molar volume, representing the dimensionless volume susceptibility in SI units. In the inset, the field dependence of the magnetization below (black line) and above (red line) T_C is shown. The arrow on the left-hand side indicates the step-like increase due to the small ordered FM moment, $M_{ord} \cong 0.05\mu_B$, obtained by extrapolating the linear $M(H)$ curve between 0.1 and 0.2 T to zero field. In determining the ordered moment, we assume that in our polycrystal the fully aligned moment dominates the magnetization at these low fields. The right-hand arrow marks an anomaly at higher field representing either the rotation of the FM moments along the magnetic hard direction or complete suppression of the Kondo screening. (b) Low-temperature specific heat plotted as C/T versus T on a logarithmic scale at zero and low values of the applied magnetic field without subtraction of any hyperfine or phononic contribution. A sharp λ-type anomaly at T_C confirms the second-order phase transition and the high quality of our sample. With increasing field, the peak broadens and transforms into a Schottky-type anomaly with a maximum at T_{Cr}.

Figure 3. (Continued) (c) Temperature dependence of the resistivity plotted as a function of T^2; dashed lines indicate the formation of a Landau–Fermi-liquid (LFL) ground state. For the sake of clarity, the different curves for $B > 0$ are shifted by $0.5\,\mu\Omega\,\mathrm{cm}$, respectively. For the zero-field curve, we additionally present data measured with a very low excitation current but less resolution (magenta curve) to demonstrate the absence of heating effects above 0.07 K. The zero-field transition at T_C (black symbol) becomes a crossover at T_{Cr} (orange stars) in finite field, shown in the inset together with the specific heat crossover temperatures (blue squares) in a B–T-phase diagram.

$\gamma_0 \cong 2000\,\mathrm{mJ\,mol^{-1}\,K^{-2}}$, reflects the existence of heavy quasi-particles with an electronic mass two to three orders of magnitude larger than the bare electron mass. Below 50 mK, the scattering of the data points significantly increases, preventing a more accurate determination of the Sommerfeld coefficient. Remarkably, C/T is larger below T_C than above the FM ordering, indicating strong fluctuations within the ferromagnetically ordered state, similar to the AFM phase in $YbRh_2Si_2$ [18]. Integrating C/T over temperature reveals an entropy gain associated with the anomaly at T_C of only about $0.02R\ln 2$. This is in accordance with the small value of the ordered moment derived from our magnetization data and provides evidence for rather weak FM order in $YbNi_4P_2$.

The onset of magnetic order is further established by the freezing out of spin-disorder scattering, i.e. a distinct reduction of the electrical resistivity at T_C, presented as ρ versus T^2 in figure 3(c). Below T_C, the resistivity follows a straight line down to the lowest measured temperatures, i.e. $\rho(T) = \rho_0 + AT^2$ with $\rho_0 \cong 2.5\,\mu\Omega\,\mathrm{cm}$ and $A \cong 52\,\mu\Omega\,\mathrm{cm\,K^{-2}}$. Therefore, all measured quantities present the hallmarks of an LFL ground state within the FM ordered phase and can be characterized by the $T \to 0$ limits of the susceptibility, χ_0, the Sommerfeld coefficient of the electronic specific heat, γ_0, and the resistivity coefficient A. The so-called Kadowaki–Woods ratio, A/γ_0^2, amounts to approximately $13\,\mu\Omega\,\mathrm{cm\,K^2\,mol^2\,J^{-2}}$, close to the universal value of $10\,\mu\Omega\,\mathrm{cm\,K^2\,mol^2\,J^{-2}}$ for heavy-fermion compounds [19]. The Sommerfeld–Wilson ratio, $W = \pi^2 k_B^2/(\mu_0\mu_{\mathrm{eff}}^2)\cdot\chi_0/\gamma_0$ with $\mu_{\mathrm{eff}} \cong 2\mu_B$, is found to be large when compared to all other heavy-fermion systems where typically values between 1 and 5 are observed [20]. In $YbNi_4P_2$, a giant value of W is observed within the ferromagnetically ordered state ($W_{T\to 0} \cong 350$) and W is still substantially enhanced well above T_C, $W_{T=0.3\,\mathrm{K}} \cong 20$. This lends further support to very strong FM quantum fluctuations in $YbNi_4P_2$.

The effect of an applied magnetic field is similar for all the presented quantities: already a small ($\cong$10 mT) magnetic field extends the LFL ground state to higher temperatures and is accompanied by a reduction of the effective mass reflected by decreased values of γ_0, A and χ_0. The field-stabilized FM state is characterized by broad crossover maxima at T_{Cr} in $\chi(T)$ and $C(T)/T$, respectively, as the Yb moments get polarized in the external field at higher temperatures (see the inset of figure 3(c)). Therefore, the system is tuned away from the QCP, in striking contrast to AFM systems, where an ordered system may be field-tuned through the QCP [3, 21, 22].

Having established the proximity of $YbNi_4P_2$ to an FM QCP, we now turn to the quantum critical regime and address the distinct deviations from the predictions of LFL theory above T_C. They are most pronounced in zero magnetic field, where $YbNi_4P_2$ is closest to the QCP. Remarkably, the specific-heat coefficient diverges stronger than logarithmically below $T = 3$ K with a power-law $C/T \propto T^{-0.42}$ down to 0.2 K. At this temperature, the classical fluctuations of

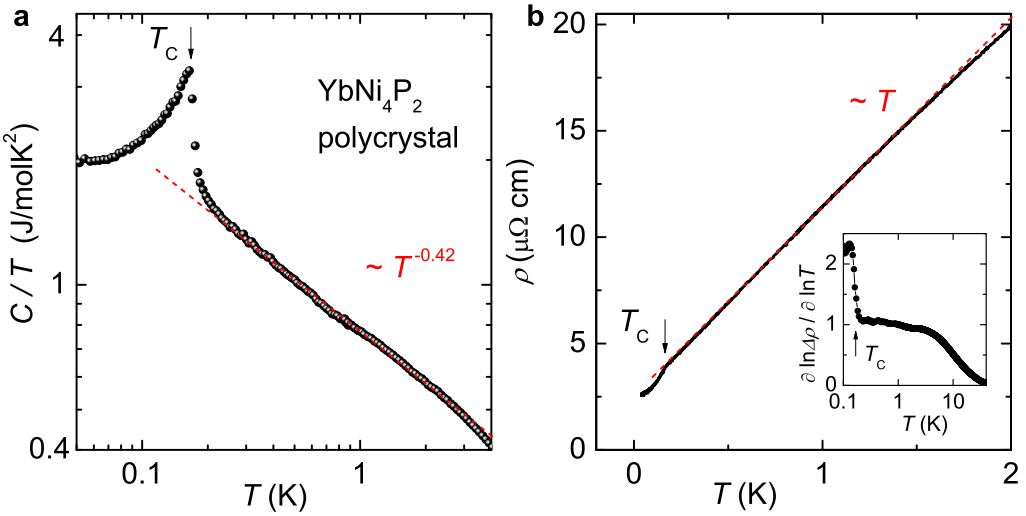

Figure 4. Pronounced non-Fermi-liquid behaviour above T_C at $B = 0$. (a) The temperature dependence of the zero-field specific heat divided by temperature in a double logarithmic representation clearly reveals a power-law divergence, $C/T \propto T^{-0.42}$, indicated by the red dashed line. (b) Linear-in-T resistivity in zero field over more than a decade in temperature. A pronounced drop at T_C precedes a T^2 law within the ordered phase. The temperature dependence of the resistivity exponent, defined as the derivative of $\ln[\Delta\rho(T)] = \ln[\rho(T) - \rho_0]$ with respect to $\ln T$, is presented in the inset.

the FM order parameter set in (see figure 4(a)). Above $T = 1$ K, there might be a crossover from a power-law to a logarithmic divergence up to $T = 7$ K, better seen in the semi-logarithmic plot of C/T versus T in figure 3(b). The resistivity follows a linear-in-T dependence for $T > T_C$, presented in figure 4(b), with a tendency to sub-linear behaviour above $T = 2$ K. For a more quantitative analysis of the resistivity exponent, we consider the logarithmic derivative, $\partial \ln(\rho - \rho_0)/\partial \ln T$. As displayed in the inset of figure 4(b), $\partial \ln(\rho - \rho_0)/\partial \ln T$ remains within the value 1.0 ± 0.1 over more than one decade in temperature above T_C before dropping above 5 K.

These strong deviations from LFL behaviour along with the low-lying FM ordering have very general implications for our current understanding of quantum phase transitions. While numerous AFM Kondo systems have been tuned towards a QCP by the variation of pressure, doping or magnetic field, appropriate candidates for the study of FM QCPs are extremely rare [3]. Starting deep inside the localized moment regime in Ce-based ferromagnets, the increase of the Kondo interaction with pressure typically leads to an AFM ground state before the QCP is reached [7]. In disordered FM 4f systems a peculiar Kondo-cluster-glass state was found, preventing the study of FM quantum criticality [23]. On the other hand, in clean itinerant FM 3d systems, it is established that no QCP exists; rather the FM transition always ends at a classical critical point (at finite T) where a first-order phase transition occurs [8, 24]. However, disorder can lead to weak signatures of FM quantum criticality as observed in various 3d alloy series [25–27], which theoretically could be explained by disorder-induced rounding effects [28]. Therefore, $YbNi_4P_2$ represents the first clean example of FM quantum criticality above a low-lying FM transition, permitting the examination of existing and the development of new theoretical predictions for the temperature dependences of the relevant

physical parameters at an FM QCP. Most theoretical work has been done in systems where the vanishing magnetism can be described within the framework of itinerant spin fluctuation theories [3]. However, our observed power laws in $C(T)/T$ and $\rho(T)$ above T_C deviate strongly from these theoretical descriptions. At present, we cannot distinguish whether these deviations result from the quasi-one-dimensionality of $YbNi_4P_2$, for which no calculations have been performed, or whether $YbNi_4P_2$ is situated close to a local QCP, where the FM transition is accompanied by a localization–delocalization transition of the f electrons. The local QCP scenario is well established for $YbRh_2Si_2$ ([29] and references therein), which presents AFM order below $T_N = 72\,\mathrm{mK}$, but nonetheless shows strong FM fluctuations in wide parts of its phase diagrams [30, 31]. We note that in $YbRh_2Si_2$, $C(T)/T$ also follows a stronger-than-logarithmically divergence below 300 mK and a linear-in-T resistivity [32]. Furthermore, a sharp λ-type transition into the antiferromagnetically ordered phase and a strongly enhanced Sommerfeld coefficient below T_N were similarly observed for $YbRh_2Si_2$ [33]. Future work has to be undertaken to tune $YbNi_4P_2$ towards the non-magnetic side of the QCP. Negative chemical pressure achieved by As substitution on the P site might be the most promising route as the stoichiometric $YbNi_4As_2$ forms in the same crystal structure but with non-magnetic Yb^{2+} ions [14] due to the much larger volume of the unit cell.

To conclude, we have discovered a new heavy-fermion Kondo-lattice system with several features that are unique among strongly correlated 4f systems. Firstly, both the crystal and the electronic structure of $YbNi_4P_2$ are quasi-1D, resulting in distinct quantum fluctuations at low temperatures. Secondly, $YbNi_4P_2$ undergoes a well-defined FM phase transition of second order at $T_C = 0.17\,\mathrm{K}$, growing out of a strongly correlated Kramers doublet ground state with a Kondo temperature, $T_K \cong 8\,\mathrm{K}$. Due to the dominant Kondo screening, only a tiny ferromagnetically ordered moment ($M_{ord} \cong 0.05\mu_B$) with a substantially reduced T_C is observed. The ferromagnetism is evidenced by a diverging susceptibility at T_C with huge absolute values comparable to established ferromagnets. The 4f spins remain strongly fluctuating down to the lowest measured temperatures, leading to a large Sommerfeld coefficient, $\gamma_0 \cong 2000\,\mathrm{mJ\,mol^{-1}\,K^{-2}}$, within the ordered phase. Above T_C, a remarkable power-law divergence of the specific heat, $C/T \propto T^{-0.42}$, and a linear-in-T resistivity are observed over more than a decade in temperature. Therefore, $YbNi_4P_2$ is the first clean system situated in the close vicinity of an FM QCP with the lowest-lying T_C ever observed among correlated systems. These FM quantum fluctuations that dominate the thermodynamic and transport properties well above T_C cannot be explained within any current theoretical framework. Furthermore, $YbNi_4P_2$ is a highly stoichiometric system and has the potential to become the prototype of an FM quantum critical material.

Acknowledgments

We sincerely thank R Weise, N Caroca-Canales and C Bergmann for assistance with sample preparation. Valuable discussions with M Baenitz, S Friedemann, A Haase, A Jesche, S Kirchner, H-H Klauß, R Küchler, N Mufti, M Nicklas, R Sarkar, J Spehling, O Stockert, U Stockert and S Wirth are gratefully acknowledged. This work was partially supported by DFG Research Unit 960 and SPP 1458.

Appendix A. Methods

The polycrystalline samples were prepared by heating a stoichiometric amount of the elements in evacuated quartz ampoules at 1000 °C for 24 h. The sample was characterized by powder and

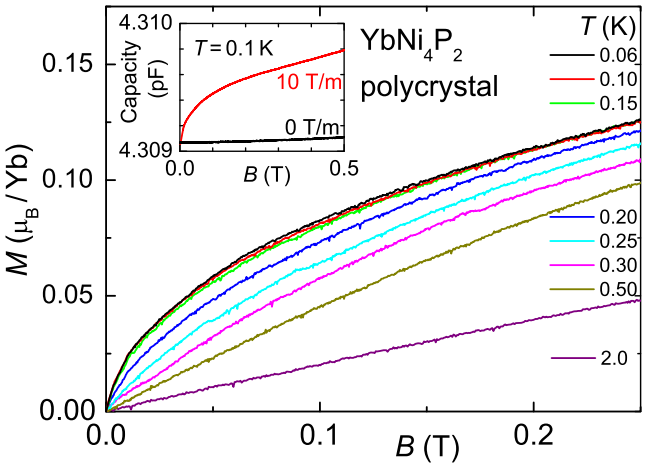

Figure A.1. Detailed magnetization measurements of $YbNi_4P_2$ at low magnetic fields for various temperatures below and above T_C. The measured capacitance at $T = 0.1$ K with an applied magnetic field gradient ($dB/dz = 10\,T\,m^{-1}$, red line) is shown in the inset together with the data measured without the field gradient (black line). The latter serves as a background signal and was subtracted to obtain the presented $M(B)$ curves.

single crystalline x-ray diffraction experiments presented in detail in appendix B. Electronic band structure calculations were performed with the full-potential non-orthogonal local-orbital minimum basis scheme FPLO code (version: FPLO 9.00-31) [34]. Within the local spin density approximation, the exchange and correlation potential of Perdew and Wang [35] has been used. The high-temperature measurements of $\rho(T)$, $S(T)$ and $C(T)$, were performed using a commercial Quantum Design PPMS equipped with a ^{3}He option. The magnetization and dc susceptibility measurements above 2 K were carried out using a Quantum Design SQUID VSM. All low-temperature measurements were carried out in ^{3}He/^{4}He dilution refrigerators. The ac susceptibility was determined at low frequencies with a modulation field amplitude of 15 μT down to 0.02 K, measured in selected static magnetic fields. Great care was taken to account for remanent fields. Above 2 K, the ac susceptibility equals the dc susceptibility determined by the SQUID VSM. The specific heat between 0.03 and 1 K was measured utilizing a semi-adiabatic heat-pulse method with the sample mounted on a silver platform. The electrical resistivity $\rho(T)$ was monitored by a standard four-point lock-in technique at 16.67 Hz down to 0.02 K.

The magnetic field dependence of the magnetization $M(B)$ was isothermally measured in a high-resolution Faraday magnetometer down to 0.06 K [36]. Background contributions from the sample platform and the torque exerted on the sample have been subtracted and were determined by measuring the capacitance without a magnetic field gradient (black line in the inset of figure A.1). However, the signal of the sample (red line in the inset of figure A.1) dominates the field dependence of the capacitance. In the main part of figure A.1, more detailed $M(B)$ curves are presented in addition to the data in the inset of figure 3(a). Below T_C, the $M(B)$ curves are nearly temperature independent but decrease strongly above T_C as expected for an FM system.

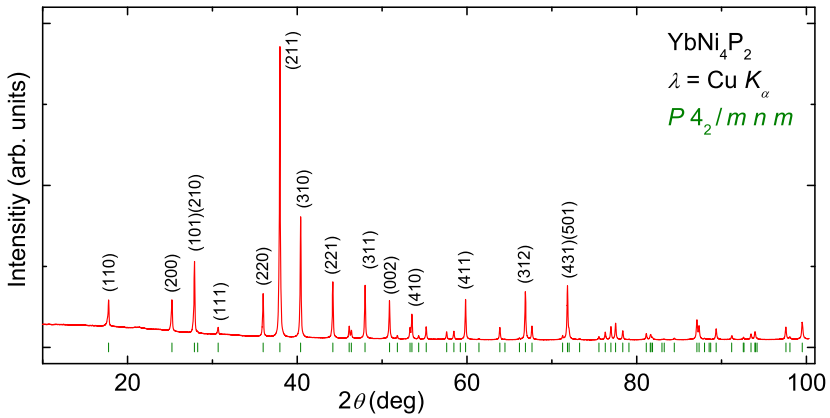

Figure B.1. Powder diffraction pattern of $YbNi_4P_2$ at room temperature. Green lines indicate the peak positions for the $P4_2/mnm$ structure type.

Table B.1. Crystallographic data and experimental details for the single crystal refinement of $YbNi_4P_2$ at room temperature. Crystallographic data: space group $P4_2/mnm$ (no. 136), $a = 7.0565(2)$ Å, $c = 3.5877(1)$ Å, $V = 178.65(1)$ Å^3 (lattice parameters were obtained from powder diffraction data), $Z = 2$, $F(000) = 424$, $U_{13} = U_{23} = 0$, $\rho_{calc} = 8.73\,g\,cm^{-3}$, $\mu(MoK\alpha) = 47.24\,mm^{-1}$ and crystal dimensions $20 \times 35 \times 65\,\mu m^3$. Collected data: MoK$\alpha$ radiation ($\lambda = 0.71073$ Å), $2\theta_{max} = 70°$, 1172 measured reflections, 238 symmetry-independent reflections, 226 observed reflections [$I > 2\sigma(I)$], $R_{int} = 0.040$, 15 parameters, $R(F) = 0.027$, $wR(F^2) = 0.059$, GooF = 1.12, numerical absorption $T_{min}/T_{max} = 0.3572$ and $\delta\rho_{min\,(max)} = -3.11\,(2.13)$ e Å^{-3}.

Atom	Site	x/a	y/a	z/c	U_{11}	U_{22}	U_{33}	U_{12}	U_{eq}
Yb	2b	0	0	0.5	0.0070(2)	U_{11}	0.0077(3)	−0.0002(1)	0.0072(2)
Ni	8i	0.3359(1)	0.0840(1)	0	0.0086(4)	0.0077(3)	0.0083(4)	−0.0008(2)	0.0082(2)
P	4g	0.2195(2)	$-x/a$	0	0.0083(5)	U_{11}	0.0076(7)	−0.0004(6)	0.0081(4)

Appendix B. X-ray diffraction

In figure B.1, we present the x-ray powder diffraction data of a polycrystalline $YbNi_4P_2$ sample recorded on an Imaging Plate Guinier Camera (Huber G670, CuKα radiation, $\lambda = 1.5406$ Å). All peaks could be indexed using the $ZrFe_4Si_2$ structure type (green lines in figure B.1), confirming the absence of any foreign phase in our sample. Unit cell parameters were refined by a least-squares procedure (the program package WinCSD [37]) using the peak positions extracted from powder patterns measured with LaB_6 as an internal standard (not shown).

Furthermore, complete structural refinement of a small single crystal was carried out on a Rigaku AFC7 diffractometer equipped with a Saturn 724+ charge-coupled device (CCD) detector using MoKα radiation. Crystallographic information and experimental details of this refinement are presented in table B.1 and were obtained using the program package ShelX [38]. The structure is in agreement with the literature [16]; however, our refinement based on single crystals is more precise than the previously reported powder data.

These crystallographic data and the refinement corroborate that $YbNi_4P_2$ is structurally highly ordered without significant crystallographic defects. For the study of quantum critical phenomena at low temperature this is an important conclusion, because disorder can often hide the intrinsic properties, in particular for materials where the dominating energy scales are small. Furthermore, the excellent stoichiometric quality of our $YbNi_4P_2$ samples is in nice agreement with the presented physical properties at low temperature, e.g. sharp anomalies at $T_C = 0.17$ K and a large residual resistivity ratio.

References

[1] Focus issue 2008 Quantum phase transitions *Nature Phys.* **4** 167–204

[2] Mathur N D, Grosche F M, Julian S R, Walker I R, Freye D M, Haselwimmer R K W and Lonzarich G G 1998 Magnetically mediated superconductivity in heavy fermion compounds *Nature* **394** 39–43

[3] Stewart G R 2001 Non-Fermi-liquid behavior in d- and f-electron metals *Rev. Mod. Phys.* **73** 797–855

[4] Park T, Ronning F, Yuan H Q, Salamon M B, Movshovich R, Sarrao J L and Thompson J D 2006 Hidden magnetism and quantum criticality in the heavy fermion superconductor $CeRhIn_5$ *Nature* **440** 65–8

[5] Friedemann S, Westerkamp T, Brando M, Oeschler N, Wirth S, Gegenwart P, Krellner C, Geibel C and Steglich F 2009 Detaching the antiferromagnetic quantum critical point from the Fermi-surface reconstruction in $YbRh_2Si_2$ *Nature Phys.* **5** 465–9

[6] Stockert O *et al* 2011 Magnetically driven superconductivity in $CeCu_2Si_2$ *Nature Phys.* **7** 119–24

[7] Süllow S, Aronson M C, Rainford B D and Haen P 1999 Doniach phase diagram, revisited: from ferromagnet to Fermi liquid in pressurized $CeRu_2Ge_2$ *Phys. Rev. Lett.* **82** 2963–6

[8] Kirkpatrick T R and Belitz D 2003 Nature of the quantum phase transition in clean itinerant Heisenberg ferromagnets *Phys. Rev.* B **67** 024419

[9] Yamamoto S J and Si Q 2010 Metallic ferromagnetism in the Kondo lattice *Proc. Natl Acad. Sci. USA* **107** 15704–7

[10] Paglione J and Greene R L 2010 High-temperature superconductivity in iron-based materials *Nature Phys.* **6** 645–58

[11] Chikhrij S I, Orishchin S V and Kuz'ma Y B 1986 New phosphides of rare-earth-metals with the $ZrFe_4Si_2$-type structure *Dopov. Akad. Nauk Ukr. SSR* A **7** 81–3

[12] Pivan J Y, Guerin R, El Ghadraoui E H and Rafiq M 1989 Tetrahedral Ni_4 clusters in a marcasite-type host structure: the preparation and crystal structure of MNi_4X_2 compounds (X = P, As; M = Zr, Hf, Y, Gd, Tb, Dy, Ho, Er, Tm, Yb, Lu) *J. Less-Common Met.* **153** 285–92

[13] Jeitschko W, Terbüchte L J, Reinbold E J, Pollmeier P G and Vomhof T 1990 Phosphides and arsenides with the $ZrFe_4Si_2$-type structure *J. Less-Common Met.* **161** 125–34

[14] Deputier S, Pena O, Le Bihan T, Pivan J Y and Guerin R 1997 Magnetic properties of the lanthanoid nickel arsenides and phosphides $LnNi_4X_2$ with $ZrFe_4Si_2$-type structure *Physica* B **233** 26–36

[15] Chikhrij S I, Gorelenko Y K, Orishchin S V, Skolozdra R V and Kuz'ma Y B 1991 Anomalous magnetic properties of $LnNi_4P_2$ phosphides *Sov. Phys.—Solid State* **33** 1556–7

[16] Kuz'ma Y B, Chykhrij S I and Budnyk S L 2000 Yb-Ni-P system *J. Alloys Compd.* **298** 190–4

[17] Köhler U, Oeschler N, Steglich F, Maquilon S and Fisk Z 2008 Energy scales of $Lu_{1-x}Yb_xRh_2Si_2$ by means of thermopower investigations *Phys. Rev.* B **77** 104412

[18] Oeschler N, Hartmann S, Pikul A P, Krellner C, Geibel C and Steglich F 2008 Low-temperature specific heat of $YbRh_2Si_2$ *Physica* B **403** 1254–6

[19] Kadowaki K and Woods S B 1986 Universal relationship of the resistivity and specific-heat in heavy-fermion compounds *Solid State Commun.* **58** 507–9

[20] Fisk Z, Ott H R and Aeppli G 1987 Experimental perspectives on heavy-electron metals *Japan. J. Appl. Phys.* **26** (Suppl. 26-3) 1882–6

[21] Heuser K, Scheidt E W, Schreiner T and Stewart G R 1998 Inducement of non-Fermi-liquid behavior with a magnetic field *Phys. Rev.* B **57** R4198–201
[22] Bud'ko S L, Morosan E and Canfield P C 2004 Magnetic field induced non-Fermi-liquid behavior in YbAgGe single crystals *Phys. Rev.* B **69** 014415
[23] Westerkamp T, Deppe M, Küchler R, Brando M, Geibel C, Gegenwart P, Pikul A P and Steglich F 2009 Kondo-cluster-glass state near a ferromagnetic quantum phase transition *Phys. Rev. Lett.* **102** 206404
[24] Chubukov A V, Pépin C and Rech J 2004 Instability of the quantum-critical point of itinerant ferromagnets *Phys. Rev. Lett.* **92** 147003
[25] Nicklas M, Brando M, Knebel G, Mayr F, Trinkl W and Loidl A 1999 Non-Fermi-Liquid behavior at a ferromagnetic quantum critical point in Ni_xPd_{1-x} *Phys. Rev. Lett.* **82** 4268–71
[26] Sokolov D A, Aronson M C, Gannon W and Fisk Z 2006 Critical phenomena and the quantum critical point of ferromagnetic $Zr_{1-x}Nb_xZn_2$ *Phys. Rev. Lett.* **96** 116404
[27] Jia S, Jiramongkolchai P, Suchomel M R, Toby B H, Checkelsky J G, Ong N P and Cava R J 2011 Ferromagnetic quantum critical point induced by dimer-breaking in $SrCo_2(Ge_{1-x}P_x)_2$ *Nature Phys.* **7** 207–10
[28] Vojta T 2003 Disorder-induced rounding of certain quantum phase transitions *Phys. Rev. Lett.* **90** 107202
[29] Friedemann S, Oeschler N, Wirth S, Krellner C, Geibel C, Steglich F, Paschen S, Kirchner S and Si Q 2010 Fermi-surface collapse and dynamical scaling near a quantum-critical point *Proc. Natl Acad. Sci. USA* **107** 14547–51
[30] Gegenwart P, Custers J, Tokiwa Y, Geibel C and Steglich F 2005 Ferromagnetic quantum critical fluctuations in $YbRh_2(Si_{0.95}Ge_{0.05})_2$ *Phys. Rev. Lett.* **94** 076402
[31] Klingner C *et al* 2011 Evolution of magnetism in $Yb(Rh_{1-x}Co_x)_2Si_2$ *Phys. Rev.* B **83** 144405
[32] Custers J, Gegenwart P, Wilhelm H, Neumaier K, Tokiwa Y, Trovarelli O, Geibel C, Steglich F, Pepin C and Coleman P 2003 The break-up of heavy electrons at a quantum critical point *Nature* **424** 524–7
[33] Krellner C, Hartmann S, Pikul A, Oeschler N, Donath J G, Geibel C, Steglich F and Wosnitza J 2009 Violation of critical universality at the antiferromagnetic phase transition of $YbRh_2Si_2$ *Phys. Rev. Lett.* **102** 196402
[34] Koepernik K and Eschrig H 1999 Full-potential nonorthogonal local-orbital minimum-basis band-structure scheme *Phys. Rev.* B **59** 1743–57
[35] Perdew J P and Wang Y 1992 Accurate and simple analytic representation of the electron–gas correlation energy *Phys. Rev.* B **45** 13244–9
[36] Sakakibara T, Mitamura H, Tayama T and Amitsuka H 1994 Faraday force magnetometer for high-sensitivity magnetization measurements at very low temperatures and high fields *Japan. J. Appl. Phys.* **33** 5067–72
[37] Akselrud L G, Zavalii P Yu, Grin Yu, Pecharsky V, Baumgartner B and Wölfel E 1993 Use of the CSD program package for structure determination from powder data *Mater. Sci. Forum* **133–136** 335–40
[38] Sheldrick G M 2008 A short history of SHELX *Acta Cryst.* A **64** 112–22